PHILOSOPHICAL TRANSACTIONS OF THE ROYAL SOCIETY A MATHEMATICAL, PHYSICAL & ENGINEERING SCIENCES

Short-Wavelength Instabilities of Riemann Ellipsoids

Norman R. Lebovitz and Alexander Lifschitz

Phil. Trans. R. Soc. Lond. A 1996 **354**, 927-950
doi: 10.1098/rsta.1996.0037

Short-wavelength instabilities of Riemann ellipsoids

By Norman R. Lebovitz[1] and Alexander Lifschitz[2]

[1]*Department of Mathematics, University of Chicago, Chicago, IL 60637, USA*
[2]*Department of Mathematics, University of Illinois, Chicago, IL 60607, USA*

Contents

Perturbations of incompressible S-type Riemann ellipsoids are considered in the limit of short wavelength. This complements the classical consideration of perturbations of long wavelength. It is shown that there is very little of the parameter space in which the laminar, steady-state flow can exist in a stable state. This confirms, in a physically consistent framework, hydrodynamic-stability results previously obtained in the context of unbounded, two-dimensional flows. The configurations stable to perturbations of arbitrarily short wavelength include the rigidly rotating configurations of Maclaurin and Jacobi, as well as a narrow continuum centred on the family of irrotational ellipsoids and including the non-rotating sphere. However, most configurations departing even slightly from axial symmetry are unstable. Some of the implications of these results for the complexity of astrophysical flows are discussed.

1. Introduction

The Riemann ellipsoids are a family of models of rotating, self-gravitating masses. As model stars they are idealized in that no account is taken of compressibility or of the complex physical processes attending stellar evolution. However, they represent essentially the only known, mathematically exact configurations of rotating stars that depart from axial symmetry. They have consequently played a consistently impor-

Phil. Trans. R. Soc. Lond. A (1996) **354**, 927–950
Printed in Great Britain

tant role in the theory of rotating stars. In particular, numerical calculations of the evolution and stability of rotating stars can often be interpreted in the framework of the theory of the equilibrium and stability of the Riemann ellipsoids. A standard reference for this theory is Chandrasekhar (1969).

The stability of the steady-state Riemann ellipsoids has been the subject of many investigations, going back to Riemann himself. Most of these investigations, including our own, are based on the linearized equations of fluid motion. Despite the long history of the subject, only small perturbations belonging to ellipsoidal harmonics of orders two, three and (in isolated cases) four have been studied with any degree of generality. As a result, very little is known about stability to perturbations of length less than, say, one-fourth the average radius. In the present paper we use the geometrical-optics approximation (Eckhoff 1981; Lifschitz & Hameiri 1991) to study stability for perturbations of arbitrarily short wavelengths, and we map the region of parameter space that is unstable to such perturbations. We restrict consideration to a subclass of the steady Riemann ellipsoids, those of type S (Chandrasekhar 1969), for which the angular velocity and vorticity of the configuration are in the same direction. There is a two-parameter family of such configurations, and the general goal of stability theory is to determine which regions of the parameter space correspond to stable configurations. The principal result of the present analysis is that almost all of the parameter space corresponds to unstable configurations. Since the S-type Riemann ellipsoids have fluid velocities with elliptical streamlines, this result is not surprising: very general instabilities of such two-dimensional flows to three-dimensional disturbances have been noted over the last decade (Pierrehumbert 1986; Bayly 1986; Craik 1989; Waleffe 1990; Bayly *et al.* 1995; see also Gledzer & Ponomarev 1992; Vladimirov & Vostretsov 1986). Those S-type ellipsoids that remain stable to perturbations of short wavelength are the classical, rigidly rotating configurations of Maclaurin and Jacobi, and a band (in parameter space) centred on the irrotational ellipsoids, i.e. those for which the total vorticity relative to inertial space vanishes. The exact extent of this band is given by inequality (5.16) below. It includes the quiescent, spherical configuration. It excludes the Dedekind family, which is of special interest in the presence of gravitational radiation.

The work of Craik (1989) is the most directly relevant to the present paper. Craik's assumptions, like those of Bayly (1986) and others who have developed the theory of instability of flows with non-circular streamlines, include that of an unbounded fluid domain, with flow velocities and pressures that also become unbounded at large distances. Under these assumptions, wave-like expressions can be found as exact solutions of the perturbation equations; indeed they remain exact for the full, nonlinear equations. It is highly plausible that the stability conclusions should carry over to *bounded* domains with *bounded* flow variables if (i) the disturbance wavelength is sufficiently small, (ii) the disturbance is localized (so the domain 'looks' unbounded from the standpoint of the perturbed region of the flow), and (iii) if the influence of the boundary can be shown to be negligible.

However, the exactness of the wave-like expressions is in general no longer possible in the context of a bounded domain like that of the Riemann ellipsoids. We verify via a WKB approximation that these expressions then become leading-order asymptotic approximations to the exact solutions of the linearized stability equations for the Riemann ellipsoids. Moreover, an energy estimate of the error enables us to give a rigorous demonstration of instability when that is the prediction of the leading-order terms. The need for this estimate can be understood from a physical

PHILOSOPHICAL TRANSACTIONS OF THE ROYAL SOCIETY A MATHEMATICAL, PHYSICAL & ENGINEERING SCIENCES

standpoint in the following way. While the leading-order terms can be localized away from the boundary, the full solution cannot be, and the effect of the boundary will ultimately be felt throughout the flow domain. The problem is therefore to show that the conclusion of instability persists despite the effect of the boundary. This is achieved mathematically via the energy estimate.

The plan of the paper is as follows. The precise assumptions and the equations to be solved are presented in §§ 2 and 3, and the WKB, or geometrical-optics, method is outlined in § 4, where the transport equations are also derived. In § 5 we consider the transport equations, which agree with the stability equations treated by Craik (1989) (see also Bayly *et al.* (1995), who considered the same system of equations, but in different physical settings). We explore certain parameter domains important in the present application analytically as well as numerically in this section. We present in § 6 the energy estimate justifying the geometrical-optics method. The results are discussed in § 7. The appendices are devoted to certain mathematical results used in § 6.

2. Assumptions and equations

The fluid mass is considered to be inviscid and of uniform density. Its evolution is therefore governed by the Euler equations of fluid dynamics,

$$\frac{D\boldsymbol{V}}{Dt} + 2\boldsymbol{\omega} \times \boldsymbol{V} = -\rho^{-1}\nabla P + \nabla(\Psi + \tfrac{1}{2}|\boldsymbol{\omega} \times \boldsymbol{x}|^2), \tag{2.1}$$

written here in a coordinate frame rotating, with respect to an inertial frame, with angular velocity $\boldsymbol{\omega}$. The uniformity of the density ρ implies the incompressibility condition,

$$\nabla \cdot \boldsymbol{V} = 0. \tag{2.2}$$

The gravitational potential Ψ is that due to the fluid mass itself:

$$\Psi(\boldsymbol{x}, t) = G \int_{D_t} \frac{\rho}{|\boldsymbol{x} - \boldsymbol{y}|} \, \mathrm{d}\boldsymbol{y}. \tag{2.3}$$

In equation (2.3) D_t represents the domain occupied by the fluid at time t. These equations must be supplemented by initial data for the velocity $\boldsymbol{V}$ as a function of position in the initial domain D_0, and boundary data on the free boundary ∂D_t. The latter consist of the kinematic condition that particles initially on the boundary remain on the boundary and the physical condition that the pressure vanish there.

To study the stability of solutions of equations (2.1), (2.2) and (2.3) we need the equations obtained from them by linearizing. We may write these as follows:

$$\frac{D\boldsymbol{u}}{Dt} + L\boldsymbol{u} + 2\Omega\boldsymbol{u} = -\nabla p + \nabla\psi, \tag{2.4}$$

$$\nabla \cdot \boldsymbol{u} = 0, \tag{2.5}$$

$$\psi(\boldsymbol{x}, t) = \frac{1}{\pi} \int_{\partial D_t} \frac{\xi_n}{|\boldsymbol{x} - \boldsymbol{y}|} \, \mathrm{d}\sigma_y, \tag{2.6}$$

where $\boldsymbol{u}$ and p represent Eulerian perturbations in velocity and pressure, ξ_n is the normal component of the Lagrangian displacement $\boldsymbol{\xi}$,

$$D/Dt \equiv \partial_t + \boldsymbol{V} \cdot \nabla, \quad L\boldsymbol{u} \equiv (\boldsymbol{u} \cdot \nabla)\boldsymbol{V} \quad \text{and} \quad \Omega\boldsymbol{u} \equiv \boldsymbol{\omega} \times \boldsymbol{u}, \tag{2.7}$$

and we have chosen the unit of time as $(\pi G\rho)^{-1/2}$. We emphasize that we consider the case when the density is spatially constant in the unperturbed configuration. Otherwise there would be a further term in the expression for the perturbation of the gravitational potential (cf. Lebovitz 1979).

The equations above mix the Lagrangian and Eulerian descriptions. A purely Lagrangian version of these equations can be found (Lebovitz 1989), which we could recover from the equations above by using the relation

$$\frac{D\boldsymbol{\xi}}{Dt} - (\boldsymbol{\xi}\cdot\nabla)\boldsymbol{V} = \boldsymbol{u} \tag{2.8}$$

between the Lagrangian displacement and the Eulerian perturbation of velocity, and one can therefore view our perturbation equations (2.4), (2.5) and (2.6) as equations for the Lagrangian displacement $\boldsymbol{\xi}$. However, it is clear that in the present context the Lagrangian displacement is irrelevant in the interior of the domain, and only its normal component at the boundary can affect the dynamics. It is therefore convenient to retain the traditional efficiency of the Eulerian description in filtering inessential particle motions and we therefore prefer the mixed description given above. This is further discussed in § 6 below where we introduce a norm for the perturbation variables $\boldsymbol{u}$ and ξ_n.

The condition of vanishing pressure on the free boundary ∂D_t, expressed in terms of the Eulerian perturbation p in the pressure, becomes

$$p|_{\partial D_t} = -\boldsymbol{\xi}\cdot\nabla P|_{\partial D_t} = |\nabla P|\xi_n|_{\partial D_t}, \tag{2.9}$$

since $\nabla P|_{\partial D_t} = -|\nabla P|\boldsymbol{n}|_{\partial D_t}$ if $\boldsymbol{n}$ is the outward normal.

3. The S-type Riemann ellipsoids

The S-type Riemann ellipsoids form a family of steady-state solutions of equations (2.1)–(2.3) for which the velocity field is a linear function of the Cartesian coordinates, and the angular velocity $\boldsymbol{\omega}$ and relative vorticity $\boldsymbol{\zeta}_{\mathrm{R}}$ are directed along the x_3 axis: $\boldsymbol{\omega} = \omega\boldsymbol{e}_3$ and $\boldsymbol{\zeta}_{\mathrm{R}} = \zeta_{\mathrm{R}}\boldsymbol{e}_3$. In a right-handed, Cartesian coordinate system aligned along the principal axes of the ellipsoid, the velocity field is

$$\boldsymbol{V} = \left(\lambda\frac{a_1}{a_2}x_2, -\lambda\frac{a_2}{a_1}x_1, 0\right). \tag{3.1}$$

Here a_1, a_2 and a_3 are the semiaxes of the ellipsoid, and λ is a parameter related to the vorticity ζ_{R} relative to the rotating frame by the formula

$$\zeta_{\mathrm{R}} = -\lambda\left(\frac{a_1}{a_2} + \frac{a_2}{a_1}\right). \tag{3.2}$$

The total vorticity relative to inertial space is given by the formula $\zeta_{\mathrm{T}} = \zeta_{\mathrm{R}} + 2\omega$. The pressure

$$P = P_0\left(1 - \frac{{x_1}^2}{{a_1}^2} - \frac{{x_2}^2}{{a_2}^2} - \frac{{x_3}^2}{{a_3}^2}\right)$$

vanishes at the surface.

A choice of semiaxes ratios $(a_2/a_1, a_3/a_1)$ determines the constants ω, λ and P_0, up to an interchange and/or a simultaneous sign change of ω and λ. The interchange of ω and λ is said to replace a configuration by its *adjoint* configuration (which has the

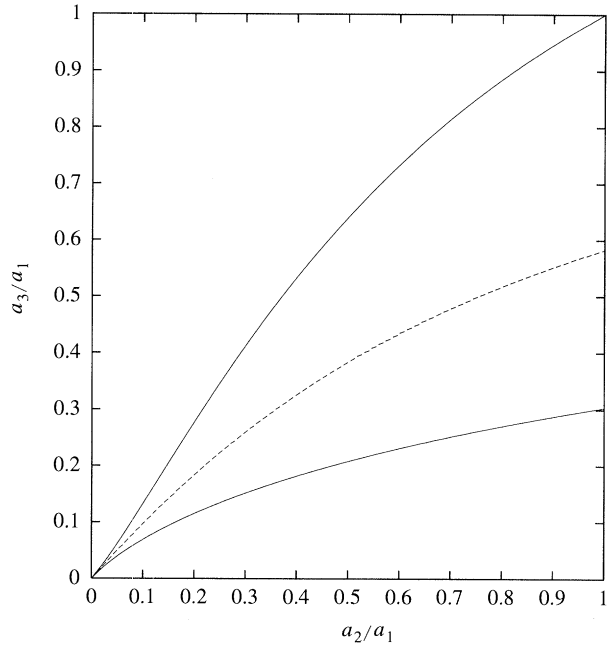

Figure 1. The region of existence of S-type ellipsoids in the $(a_2/a_1, a_3/a_1)$ plane is bounded by the solid curves. The dashed curve represents the family of Jacobi ellipsoids (among the direct configurations) and the family of Dedekind ellipsoids (among the adjoint configurations).

same shape but a different velocity field). We may assume, without loss of generality, that $\omega \geqslant 0$. Not all choices of semiaxes ratios correspond to steady-state ellipsoids of the kind described. The admissible configurations are found to occupy a certain horn-shaped region (see figure 1) in the unit square of the $(a_2/a_1, a_3/a_1)$ plane. On the other hand, the parameter

$$f \equiv \zeta_{\mathrm{R}}/\omega = -\frac{\lambda}{\omega}\left(\frac{a_1}{a_2} + \frac{a_2}{a_1}\right) \tag{3.3}$$

takes all real values, extended to include $\pm\infty$. A given choice of f specifies a curve in the admissible domain of the $(a_2/a_1, a_3/a_1)$ plane. For example, the choice $f = -2$ specifies a family of ellipsoids each of which has total vorticity $\zeta_{\mathrm{T}} = 0$. For the Maclaurin spheroids $(a_1 = a_2)$ the choice of the pair (ω, λ) is ambiguous and so, therefore is the choice of f. This ambiguity is resolved by regarding an axisymmetric figure as a limit of a non-axisymmetric family with a fixed value of f. The related parameter $x = -\lambda/\omega$ is also useful: replacing x by $1/x$ corresponds to replacing a configuration by its adjoint. We shall refer to configurations for which $-1 < x < +1$ as *direct* configurations, and those for which $x < -1$ or $x > +1$ as *adjoint* configurations. Those for which $x = \pm 1$ are *self-adjoint*. Details may be found in Chandrasekhar (1969).

4. The geometrical-optics approximation

For perturbations of arbitrarily small spatial scale we shall seek solutions of equations (2.4)–(2.6) in the form (cf. Eckhoff 1981 and Lifschitz & Hameiri 1991 for

a fuller description of this method) of the geometrical-optics approximation with remainder,

$$\boldsymbol{u}(\boldsymbol{x},t,\epsilon) = \mathrm{e}^{\mathrm{i}\Phi(\boldsymbol{x},t)/\epsilon}\{\boldsymbol{u}^{(0)}(\boldsymbol{x},t) + \epsilon\boldsymbol{u}^{(1)}(\boldsymbol{x},t)\} + \epsilon\boldsymbol{u}^{r}(\boldsymbol{x},t,\epsilon), \tag{4.1}$$

$$p(\boldsymbol{x},t,\epsilon) = \mathrm{e}^{\mathrm{i}\Phi(\boldsymbol{x},t)/\epsilon}\{p^{(0)}(\boldsymbol{x},t) + \epsilon p^{(1)}(\boldsymbol{x},t))\} + \epsilon p^{r}(\boldsymbol{x},t,\epsilon), \tag{4.2}$$

where ϵ $(0 < \epsilon \ll 1)$ measures the spatial scale, Φ is a real-valued function, and $\boldsymbol{u}^{(j)}, p^{(j)}$ $(j = 0, 1, r)$ are complex-valued. A similar representation

$$\boldsymbol{\xi}(\boldsymbol{x},t,\epsilon) = \mathrm{e}^{\mathrm{i}\Phi(\boldsymbol{x},t)/\epsilon}\{\boldsymbol{\xi}^{(0)}(\boldsymbol{x},t) + \epsilon\boldsymbol{\xi}^{(1)}(\boldsymbol{x},t)\} + \epsilon\boldsymbol{\xi}^{r}(\boldsymbol{x},t,\epsilon) \tag{4.3}$$

may be assumed for the Lagrangian displacement. This in turn induces a decomposition of the perturbation ψ of the gravitational potential into three terms. As we shall see below, we are free to choose $\boldsymbol{\xi}^{(0)}$ and $\boldsymbol{\xi}^{(1)}$ to vanish at the boundary of D; this will then leave only the remainder term

$$\psi(\boldsymbol{x},t,\epsilon) = \epsilon\psi^{r}(\boldsymbol{x},t,\epsilon) = \frac{1}{\pi}\int_{\partial D_t} \frac{\epsilon\xi_n^r}{|\boldsymbol{x}-\boldsymbol{y}|}\,\mathrm{d}\sigma_y$$

for the perturbation of the gravitational potential.

Substitution of these expressions into equations (2.4) and (2.5) above leads in a straightforward way to the following equations:

$$\frac{D\Phi}{Dt}\boldsymbol{u}^{(0)} + p^{(0)}\boldsymbol{k} = 0, \tag{4.4}$$

$$\frac{D\boldsymbol{u}^{(0)}}{Dt} + (L+2\Omega)\boldsymbol{u}^{(0)} + \nabla p^{(0)} = -\mathrm{i}\left(\frac{D\Phi}{Dt}\boldsymbol{u}^{(1)} + p^{(1)}\boldsymbol{k}\right), \tag{4.5}$$

$$\frac{D\boldsymbol{u}^{r}}{Dt} + (L+2\Omega)\boldsymbol{u}^{r} + \nabla p^{r} - \nabla\psi^{r} = -\mathrm{e}^{\mathrm{i}\Phi/\epsilon}\{D\boldsymbol{u}^{(1)}/Dt + (L+2\Omega)\boldsymbol{u}^{(1)} + \nabla p^{(1)}\}, \tag{4.6}$$

from the linearized Euler equations, and

$$\boldsymbol{k}\cdot\boldsymbol{u}^{(0)} = 0, \tag{4.7}$$

$$\nabla\cdot\boldsymbol{u}^{(0)} = -\mathrm{i}\boldsymbol{k}\cdot\boldsymbol{u}^{(1)}, \tag{4.8}$$

$$\nabla\cdot\boldsymbol{u}^{r} = -\mathrm{e}^{\mathrm{i}\Phi/\epsilon}\nabla\cdot\boldsymbol{u}^{(1)}, \tag{4.9}$$

from the linearized continuity equation. In these equations we have used the notation

$$\boldsymbol{k} \equiv \nabla\Phi. \tag{4.10}$$

Equation (4.4) is satisfied compatibly with equation (4.7) if

$$\frac{D\Phi}{Dt} = 0 \quad \text{and} \quad p^{(0)} = 0. \tag{4.11}$$

Equation (4.5) now implies

$$\frac{D\boldsymbol{u}^{(0)}}{Dt} + (L+2\Omega)\boldsymbol{u}^{(0)} - |\boldsymbol{k}|^{-2}\boldsymbol{k}\cdot\left\{\frac{D\boldsymbol{u}^{(0)}}{Dt} + (L+2\Omega)\boldsymbol{u}^{(0)}\right\}\boldsymbol{k} = 0.$$

This equation can be reduced to an ordinary differential equation for $\boldsymbol{u}^{(0)}$ as follows (cf. Lifschitz & Hameiri 1991). Differentiating equation (4.7) we find

$$\boldsymbol{k}\cdot\frac{D\boldsymbol{u}^{(0)}}{Dt} = -\frac{D\boldsymbol{k}}{Dt}\cdot\boldsymbol{u}^{(0)},$$

and differentiating $\boldsymbol{k}$ we find, with the aid of the first of equations (4.11),

$$\frac{D\boldsymbol{k}}{Dt} = -L^t\boldsymbol{k}, \tag{4.12}$$

where L^t is the transpose of the matrix L. We'll refer to this equation, which plays a significant role in the analysis, as the *eikonal* equation. Together with the preceding equation, it reduces the expression for $p^{(1)}$ to a linear expression in $\boldsymbol{u}^{(0)}$, and equation (4.5) now takes the form

$$\frac{D\boldsymbol{u}^{(0)}}{Dt} = B\boldsymbol{u}^{(0)}, \tag{4.13}$$

where

$$B\boldsymbol{u} = -(L+2\Omega)\boldsymbol{u} + 2|\boldsymbol{k}|^{-2}\{\boldsymbol{k}\cdot((L+\Omega)\boldsymbol{u})\}\boldsymbol{k}. \tag{4.14}$$

We'll refer to equation (4.13) as the *transport* equation. It is straightforward to show that the incompressibility condition (4.7) holds for $t > 0$ in consequence of this equation if it holds at the initial instant. In Lagrangian representation $\boldsymbol{x} = \boldsymbol{X}(\boldsymbol{x}_0, t)$, this is an ordinary differential equation.

More precisely, the equations for the unperturbed Lagrangian orbits, $\mathrm{d}\boldsymbol{x}/\mathrm{d}t = \boldsymbol{u}(\boldsymbol{x}, t)$, together with the eikonal and transport equations, form a system of ordinary differential equations in time, with initial data $\boldsymbol{x}_0$, $\boldsymbol{k}_0$, $\boldsymbol{u}_0^{(0)}$, which can be supplied sequentially. Therefore, in the general case, the matrix B depends parametrically on both $\boldsymbol{x}_0$ (through its dependence on L) and on $\boldsymbol{k}_0$ (in our present application it happens that L is independent of x, so there is no dependence of B or of $\boldsymbol{k}$ on $\boldsymbol{x}_0$).

As described in previous applications of the geometrical-optics method in fluid dynamics, the leading-order approximations can be localized, in the following sense: initial data can be chosen so that the leading-order terms (those with superscripts 0 and 1) are different from zero only on a chosen tube of streamlines. More particularly, suppose initial data $\boldsymbol{u}^{(0)} = \boldsymbol{0}$ are given for a particular value of $\boldsymbol{x}_0$ in D. Then $\boldsymbol{u}^{(0)} = \boldsymbol{0}$ for all $t > 0$ and the same value of $\boldsymbol{x}_0$, i.e. along the streamline passing through $\boldsymbol{x}_0$. By choosing initial data vanishing outside a chosen set of streamlines, we localize the perturbation velocity on those streamlines, in leading order. For the components $(\boldsymbol{u}^{(1)}, p^{(1)})$ we may write (cf. equations (4.5), (4.8))

$$\boldsymbol{u}^{(1)} = \mathrm{i}|\boldsymbol{k}|^{-2}\boldsymbol{k}\nabla\cdot\boldsymbol{u}^{(0)},$$

$$p^{(1)} = \mathrm{i}|\boldsymbol{k}|^{-2}\boldsymbol{k}\cdot\left\{\frac{D\boldsymbol{u}^{(0)}}{Dt} + (L+2\Omega)\boldsymbol{u}^{(0)}\right\},$$

which are again localized if $\boldsymbol{u}^{(0)}$ is.

Suppose in particular that $\boldsymbol{u}^{(0)} = \boldsymbol{u}^{(1)} = \boldsymbol{0}$ on ∂D at time $t = 0$. Then they remain zero on the boundary for all $t > 0$. On the other hand, referring to equations (4.3) and (4.11), we see that $\boldsymbol{\xi}^{(i)}$ and $\boldsymbol{u}^{(i)}$ are related by equation (2.8), $(i = 0, 1)$. If we require that $\boldsymbol{\xi}^{(0)}$ and $\boldsymbol{\xi}^{(1)}$ vanish on ∂D at $t = 0$, then they also vanish there for all $t > 0$. This implies that $\psi = \psi^r$, justifying our earlier assumption.

The temporal behaviour of the leading-order approximation is found by solving equation (4.13). Unbounded solutions suffice to prove instability, provided the remainder terms $(\boldsymbol{u}^r, p^r)$ can be shown incapable of cancelling the growth of the leading-order terms. For this it is enough, as Eckhoff (1981) and Lifschitz & Hameiri (1991) have pointed out, if the temporal growth of the remainder terms in an appropriate norm (cf. § 6) is bounded, not necessarily in time, but uniformly in ϵ. For

then the inequality

$$||(\boldsymbol{u},p)|| \geqslant ||(\boldsymbol{u}^{(0)},p^{(0)})|| - \epsilon\{||(\boldsymbol{u}^{(1)},p^{(1)})|| + ||(\boldsymbol{u}^{r},p^{r})||\}$$

implies that if the leading-order approximation grows without bound for some choice of arbitrarily small initial data compatible with the incompressibility condition (4.7), then the full solution exceeds in norm any fixed bound, for arbitrarily small initial data. The key estimate controlling the growth of $(\boldsymbol{u}^r, p^r)$ is inequality (6.4).

The representation (4.1)–(4.3) need not remain uniformly valid in time for all $t > 0$ when ϵ is fixed. From the standpoint of formal asymptotic expansions this means the expansion may eventually become 'disordered'; from the standpoint of physics it means that the influence of the boundary may not be negligible permanently. However, the energy estimate of § 6 shows that the expansion is uniformly valid in ϵ for each fixed $t > 0$, and this is sufficient to conclude that if the leading-order expressions are temporally unbounded, then so is the full solution, for sufficiently small ϵ.

Temporally *bounded* solutions of equation (4.13) fail to prove stability, on two grounds: (i) the error term may be unbounded and (ii) even if it is bounded, only a limited class of perturbations is under consideration. On this understanding, we nevertheless refer for brevity to bounded solutions of the transport equations as stable.

5. Analysis of stability

In the present section we specialize the geometrical-optics equations derived in § 4 for the case of the S-type Riemann ellipsoids and analyze their solutions. The stability equations are equivalent to those studied, in more general parameter regimes, by Craik (1989) and by Bayly *et al.* (1995). Here we not only restrict the parameters to those appropriate to the Riemann ellipsoids but also emphasize physically significant subregions of the allowed parameter space.

(*a*) *Formulation*

The matrices L and Ω take the forms (cf. equation (2.7) above)

$$L = \begin{pmatrix} 0 & \lambda a_1/a_2 & 0 \\ -\lambda a_2/a_1 & 0 & 0 \\ 0 & 0 & 0 \end{pmatrix} \quad \text{and} \quad \Omega = \begin{pmatrix} 0 & -\omega & 0 \\ \omega & 0 & 0 \\ 0 & 0 & 0 \end{pmatrix}. \tag{5.1}$$

The matrix Ω is always independent of position, whereas the matrix L is independent of position in the present case because the underlying flow is linear in the coordinates. Both are constants because the unperturbed flow is steady.

Several useful conclusions can be drawn very simply from the structure of equations (4.13) and (5.1). We henceforth write $\boldsymbol{b}$ in place of $\boldsymbol{u}^{(0)}$, and denote its complex conjugate by $\boldsymbol{b}^*$. Taking the scalar product of each side of equation (4.13) with $\boldsymbol{b}^*$, and noting that the incompressibility condition (4.7) holds with real $\boldsymbol{k}$, we find after a short calculation that

$$\frac{\mathrm{d}}{\mathrm{d}t}|\boldsymbol{b}|^2 = -\lambda\left(\frac{a_1}{a_2} - \frac{a_2}{a_1}\right)(b_1^* b_2 + b_1 b_2^*).$$

If $\lambda = 0$ (the Jacobi family) or if $a_2 = a_1$ (the Maclaurin family) the right hand side

vanishes and the amplitude of the Eulerian velocity field is conserved. We therefore conclude that these classical, rigidly rotating configurations are stable to disturbances of short wavelength. More generally, since the final factor on the right-hand side is not greater than $|\boldsymbol{b}|^2$, the preceding equation provides an upper bound on the growth rate of any instability:

$$\frac{\mathrm{d}}{\mathrm{d}t}|\boldsymbol{b}|^2 \leqslant |\lambda|\left(\frac{a_1}{a_2}-\frac{a_2}{a_1}\right)|\boldsymbol{b}|^2. \tag{5.2}$$

If the flow determined by L above is decomposed into a rotation with vorticity ζ_{R} and a deformation with strain rate ε (cf. Waleffe 1990), one finds

$$\varepsilon = \frac{\lambda}{2}\left(\frac{a_1}{a_2}-\frac{a_2}{a_1}\right).$$

Hence the growth rate of $\boldsymbol{b}$ is limited by the strain rate.

It is also convenient to decompose three-vectors into a scalar component parallel to the x_3 axis and a two-vector component parallel to the (x_1, x_2) plane; below we denote these components by the subscripts $\|$ and $\perp$ and refer to them as vertical and horizontal components respectively. In this notation the full system of geometrical-optics equations for the S-type Riemann ellipsoids becomes

$$\frac{\mathrm{d}\boldsymbol{k}_\perp}{\mathrm{d}t} = -L_\perp{}^t\boldsymbol{k}_\perp, \quad \frac{\mathrm{d}k_\|}{\mathrm{d}t} = 0, \tag{5.3}$$

$$\frac{\mathrm{d}\boldsymbol{b}_\perp}{\mathrm{d}t} = B_\perp\boldsymbol{b}_\perp, \quad \frac{\mathrm{d}b_\|}{\mathrm{d}t} = \boldsymbol{\beta}\cdot\boldsymbol{b}_\perp. \tag{5.4}$$

The matrices bearing the subscript $\perp$ represent the upper two-by-two blocks of the corresponding matrices without the subscripts (cf. equations (4.12), (4.13) and (5.1)).

The general solution of equation (5.3) is (cf. Bayly 1986; Craik & Criminale 1986)

$$\boldsymbol{k} = k_0\left(\left(\frac{2a_2^2}{a_1^2+a_2^2}\right)^{1/2}(1-\mu^2)^{1/2}\cos\phi, -\left(\frac{2a_1^2}{a_1^2+a_2^2}\right)^{1/2}(1-\mu^2)^{1/2}\sin\phi, \mu\right). \tag{5.5}$$

Here $\phi = \lambda t + \phi_0$ and μ represents the ratio of k_3 to the norm of $\boldsymbol{k}$ at a particular instant. The factor k_0 representing the amplitude of the wave-vector may, without loss of generality, be set equal to one (note that the vector field determining $\boldsymbol{b}$, equation (5.4), is homogeneous of degree zero in $\boldsymbol{k}$). In order to satisfy the incompressibility condition (4.7) above, it is necessary and sufficient to restrict initial data for the system (5.4) to the manifold $\boldsymbol{b}\cdot\boldsymbol{k} = 0$. It is sufficient to study the equation for the horizontal components of $\boldsymbol{b}$ since its vertical component can be determined from the incompressibility condition (Craik 1989).

It is convenient to introduce the transformations (Bayly *et al.* 1995)

$$\begin{pmatrix} c_1 \\ c_2 \end{pmatrix} = (k/k_\perp)\begin{pmatrix} k_1 & k_2 \\ -k_2 & k_1 \end{pmatrix}\begin{pmatrix} b_1 \\ b_2 \end{pmatrix}, \quad \tau = 2(\lambda t + \phi_0). \tag{5.6}$$

We further take as parameters, in place of $(\mu, a_2/a_1, a_3/a_1)$ the triple (μ, δ, f), where f is as previously defined (equation (3.3) above) and

$$\delta = \frac{{a_1}^2 - {a_2}^2}{{a_1}^2 + {a_2}^2}. \tag{5.7}$$

In place of equation (5.4) for $\boldsymbol{b}_\perp$ we obtain

$$\frac{\mathrm{d}\boldsymbol{c}}{\mathrm{d}t} = N\boldsymbol{c}, \tag{5.8}$$

which is in Hamiltonian form with

$$N = \begin{pmatrix} \dfrac{\mathrm{d}}{\mathrm{d}\tau}\log\sqrt{\dfrac{1-\delta\cos\tau}{1-(1-\mu^2)\delta\cos\tau}} & -\dfrac{\mu^2(f(1-\delta^2)+2(1-\delta\cos\tau))}{f\sqrt{1-\delta^2}(1-\delta\cos\tau)(1-(1-\mu^2)\delta\cos\tau)} \\ \dfrac{(2+f)}{f\sqrt{1-\delta^2}} & -\dfrac{\mathrm{d}}{\mathrm{d}\tau}\log\sqrt{\dfrac{1-\delta\cos\tau}{1-(1-\mu^2)\delta\cos\tau}} \end{pmatrix}. \tag{5.9}$$

Since the transformation from $\boldsymbol{b}_\perp$ to $\boldsymbol{c}$ is periodic in time, the stability properties of the systems (5.4) and (5.8) are the same. Since the matrix $N = N(\tau, \mu, \delta, f)$ is analytic in the parameters for $|\mu| \leqslant 1, |\delta| < 1, |f| > 0$, so also are any solutions with analytic initial data. In fact N depends only on μ^2 and, without loss of generality. we restrict consideration below to the interval $0 \leqslant \mu \leqslant 1$.

The matrix N is 2π-periodic in τ so we can use standard Floquet theory to address the stability problem. Let $\Phi(\tau)$ be the fundamental matrix solution of equation (5.8) reducing to the identity at $\tau = 0$, and $M = \Phi(2\pi)$ be the corresponding monodromy matrix. Since $\det M \equiv 1$ (this follows immediately from the vanishing of the trace of N), the eigenvalues of M satisfy the equation,

$$\nu^2 - \Delta\nu + 1 = 0, \tag{5.10}$$

where the discriminant $\Delta = \operatorname{tr} M$ is an analytic function of (μ, δ, f). It is clear (cf. Bayly 1986; Craik 1989; Magnus & Winkler 1979) that one of the roots is real and exceeds unity in absolute value if $|\Delta| > 2$. This is the criterion for exponential instability. We infer stability if $|\Delta| < 2$, whereas, in the borderline case $|\Delta| = 2$, we may have stability (if M is diagonal) or algebraic instability (if it is not).

A complete picture, in the space of parameters f, μ and δ, of the stability of the S-type ellipsoids, relies on numerical computations of the discriminant Δ, but certain cases of special interest are easily treated exactly with the aid of equations (5.8) and (5.9).

(*b*) *Special values of* μ, f *and* δ

If $\mu = 0$ (Bayly *et al.* 1995) we anticipate stability in conformity to the general conclusion that planar flows with elliptical streamlines are unstable only to disturbances out of the plane. In this case N reduces to a Jordan block and the system of equations is easily solved to give $\Delta(0, \delta, f) = 2$. Although this condition does not exclude algebraic instability the incompressibility condition guarantees that the latter does not occur. Thus, every S-type ellipsoid is stable to perturbations propagating only in the horizontal plane. It is only in this case that the incompressibility condition needs to be taken explicitly into account. A perturbation analysis valid for $f \neq 0$ shows that stability persists for small μ.

If $\mu = 1$ (Craik 1989), the transformation (5.6) is formally singular, but the matrix N is well-defined, and an independent analysis confirms that

$$\Delta(1, \delta, f) = 2\cos(2\upsilon\pi), \tag{5.11}$$

where

$$\upsilon = \frac{1}{2f}\sqrt{\left(f + \frac{4}{1+\delta}\right)\left(f + \frac{4}{1-\delta}\right)}.$$

Accordingly, all the configurations such that

$$-\frac{4}{1-\delta} < f < -\frac{4}{1+\delta} \tag{5.12}$$

are unstable. The endpoints of this interval, where $|\Delta(1, \delta, f)| = 2$, play a special role in the subsequent analysis. The value $f = -4$, which lies roughly in the middle, can be shown to be the value at which the maximum growth rate, as given by inequality (5.2), is attained.

If $f = 0$ we know from inequality (5.2) that these (Jacobi) figures are stable; a straightforward perturbation analysis shows that stability is lost for small $f \neq 0$.

If $f = -2$, i.e. if the total vorticity $\zeta_{\mathrm{T}} = 0$, then $N_{21} = 0$, and the system (5.8) can again be integrated in elementary functions. The fundamental solution is periodic in time,

$$\Delta(\mu, \delta, -2) = 2, \tag{5.13}$$

and therefore the family of irrotational ellipsoids is stable. Moreover, a perturbation analysis shows that configurations sufficiently near the irrotational family are stable. The actual extent of this irrotational band has been determined by a combination of numerical and analytic calculations, and is indicated in figures 2 and 5 below and by equation (5.16). It is a concrete realization of the stabilization in rotating systems discussed by Craik (1989) and, in a different context, by Bayly *et al.* (1995).

If $\delta = 0$, i.e. the ellipsoid is a member of the Maclaurin family, the matrix N is time-independent and the discriminant Δ can be found explicitly. We easily find

$$\Delta(\mu, 0, f) = 2\cos(2\eta\pi), \tag{5.14}$$

where $\eta = \mu(2 + f)/f$. According to equation (5.14) $|\Delta| \leqslant 2$ for all Maclaurin spheroids, whereas, in the limiting cases when $|\Delta| = 2$, evaluation of the monodromy matrix M shows it to be diagonal, implying stability in all cases, agreeing with our earlier conclusion.

If for some value of f we find that $|\Delta(\mu, 0, f)|$ is strictly less than two for all values of μ in the interval $[0, 1]$, then for that value of f the same is true of $|\Delta(\mu, \delta, f)|$ for small enough δ, and we can conclude that nearby S-type ellipsoids with this value of f are stable. This will be the case if $2\eta \neq 0, \pm 1, \pm 2, \ldots$ for any μ in $[0, 1]$. Now, $2\eta = 0$ only if $\mu = 0$ (for arbitrary f) or if $f = -2$ (for arbitrary μ), and we have stability in each of these cases, as previously noted. A simple calculation shows that 2η cannot take on any other integer values if

$$-4 < f < -4/3; \tag{5.15}$$

this implies that $|\Delta(\mu, 0, f)| < 2$ and these f-values therefore label those Riemann sequences whose near-axisymmetric members are stable to disturbances of short wavelength. For any value of f outside this interval, the corresponding Riemann sequence is a candidate for having nearly axisymmetric, unstable members. A perturbation analysis which is omitted for the sake of brevity shows that every candidate in fact has such unstable members.

PHILOSOPHICAL TRANSACTIONS OF THE ROYAL SOCIETY A MATHEMATICAL, PHYSICAL & ENGINEERING SCIENCES

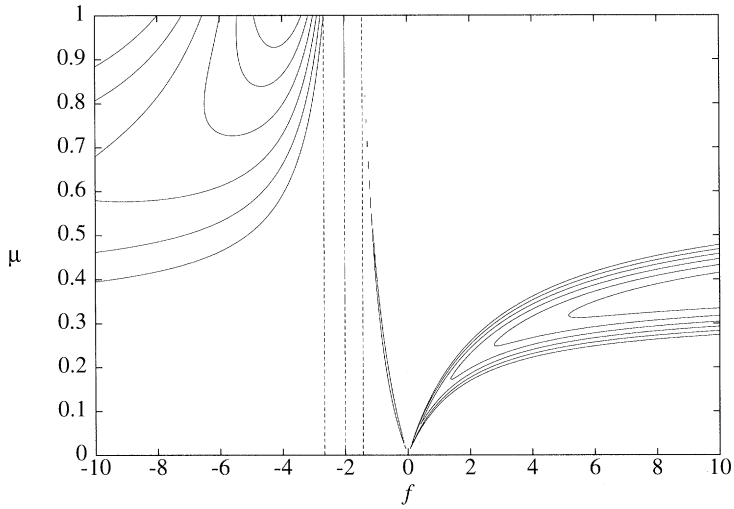

Figure 2. The strip $0 \leqslant \mu \leqslant 1, -10 < f < 10$ for $\delta = 0.5$. The widest of the instability tongues are shown. The stable configurations are those that are stable for each μ, i.e. for each wave-vector orientation. These are seen to occupy a band bounded by vertical, dashed lines that straddle the vertical line $f = -2$. The curves lying inside the instability tongues represent level sets of the discriminant. Note that the instability tongue immediately right of the right-hand dashed line is very narrow and therefore incompletely resolved in this diagram. The larger instability domains to the left and right, when extended to $f = \pm\infty$, merge, forming a single tongue.

(*c*) *Synthesis*

Combining our analytical and asymptotic results with a numerical study of the behaviour of the discriminant $\Delta(\mu, \delta, f)$, we arrive at a rather complete picture of the stability and instability domains. In particular, for a fixed positive value of δ, we indicate in figure 2 the instability domains in the (μ, f) strip. Our figure 2 should be compared with figure 2 of Craik (1989) and figure 6 of Bayly *et al.* (1995); note that in these papers $g = 2/f$ is used as an independent variable. It appears from this figure that the stabilizing effect can be predicted solely via the analysis for $\mu = 1$, i.e. for perturbations propagating along the vertical axis of the ellipsoid. The principal interval of instability at the top of figure 2 corresponds to values of f making $\upsilon^2 < 0$ (inequality (5.12)). The f-interval of stability is bounded on the left by this instability interval, and on the right by next point where $|\Delta| = 2$. There are no instability tongues intersecting the line $\mu = 0$ according to this figure, except at $f = 0$. This conforms to the asymptotic result mentioned in § 5 *b* that stability persists for small μ. One can now conclude from these remarks that the S-type ellipsoids are stable with respect to three-dimensional perturbations if and only if the ellipticity δ and relative vorticity f satisfy the inequality

$$-\frac{4}{1+\delta} \leqslant f \leqslant -\frac{4}{1+\sqrt{4-3\delta^2}}. \tag{5.16}$$

All other ellipsoids are unstable: the stable Jacobi ellipsoids lie at $f = 0$ in this figure, and the stable Maclaurin spheroids are found in the limit when $\delta \to 0$ and the instability tongues collapse to curves on which $|\Delta| = 2$. The stabilizing effect is rather subtle: the midpoint of stable ellipsoids is at $f = -2$ while the most unstable ellipsoids have $f = -4$.

PHILOSOPHICAL TRANSACTIONS OF THE ROYAL SOCIETY A MATHEMATICAL, PHYSICAL & ENGINEERING SCIENCES

We now reformulate our results in terms of the original variables a_2/a_1 and a_3/a_1 rather than the ellipticity δ and relative vorticity f. Above we fixed δ, $0 \leqslant \delta < 1$, and varied f, $-\infty < f < \infty$. Now we can imagine fixing a_2/a_1 and varying a_3/a_1 within the limits determined by the existence conditions, represented by the upper and lower boundaries in figure 1 above and figure 5 below. For comparison with figure 2 it may be helpful to observe the following. For the adjoint configurations the parameter f varies from $(a_1^2 + a_2^2)/a_1 a_2$ (on the lower boundary of the existence region) to $+\infty$ (on the Dedekind line), and then from $-\infty$ to $-(a_1^2 + a_2^2)/a_1 a_2$ (on the upper boundary of the existence region). For the direct configurations f varies smoothly from the same values at boundaries through zero (on the Jacobi line).

The stability domains in the $(\mu, a_3/a_1)$ plane are represented in figures $3a, b$. Figure $3a$ presents these domains for the direct and adjoint configurations and a representative choice of a_2/a_1, namely 0.7. Only a small interval of a_3/a_1 at the far right of the figure is stable to wavevectors of all orientations. Outside this interval there is for each choice of a_3/a_1 a band of wave-vectors corresponding to growing amplitude, except for the stable Jacobi configuration visible at $a_3/a_1 = 0.478$. The stable interval is seen from the diagram to be determined by $\mu = 1$, as already noted; this has been a useful check on the numerics. Figure $3b$ provides the same information when $a_2/a_1 = 0.3$. Note that the stability interval for the adjoint configurations has disappeared in figure $3b$.

Figure $4a, b$ shows the growth rates of short wavelength instabilities, maximized over all possible orientations of the wave-vector ($0 \leqslant \mu \leqslant 1$), of the direct and adjoint configurations, for the same choices of parameters as in figure 3. We note that the instabilities of the adjoint configurations typically grow much more rapidly than do those of the direct configurations. Bounds for the growth rates are given by inequality (5.2) above. The regions of stability and instability to short wavelength perturbations in the $(a_2/a_1, a_3/a_1)$ plane for the direct and adjoint configurations are indicated in figures $5a$ and b respectively. The band of stability is seen to occupy only a small fraction of the parameter space; the much larger region of instability abuts the line of Maclaurin spheroids, except near the region where the latter tend to a sphere. Consequently, for Maclaurin spheroids lying outside this small region, the smallest departure from axial symmetry implies the instability of the corresponding motion.

6. The energy estimate

In this section we show that a conclusion of instability on the basis of the geometrical-optics procedure used above is mathematically firm. The considerations of this section do not require the unperturbed configuration to be steady and can therefore be used in subsequent applications to time-dependent flows. Accordingly, we allow the domain $D = D_t$, the velocity $\boldsymbol{V} = \boldsymbol{V}(\boldsymbol{x}, t)$ and the pressure $P = P(\boldsymbol{x}, t)$ to depend on time; the density ρ could also depend on time but we continue to assume that it is spatially uniform.

We introduce the energy-like functional E, defined as follows:

$$E(\boldsymbol{\xi}) = \frac{1}{2}\int_{D_t} |\boldsymbol{u}(\boldsymbol{x}, t)|^2 \, \mathrm{d}\boldsymbol{x} + \frac{1}{2}\int_{\partial D_t} |\nabla P||\xi_n|^2 \, \mathrm{d}\sigma, \tag{6.1}$$

where the second integral is extended over the boundary of the domain D_t. The square-root of this functional is a seminorm, as opposed to a norm, for the La-

(*a*)

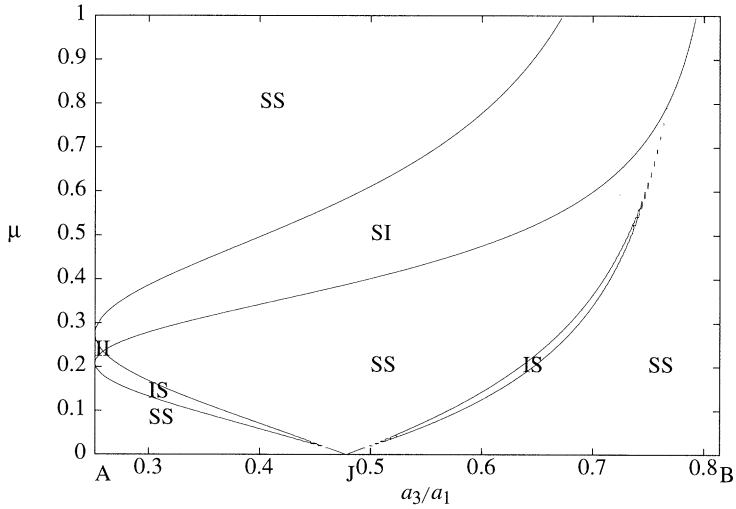

(*b*)

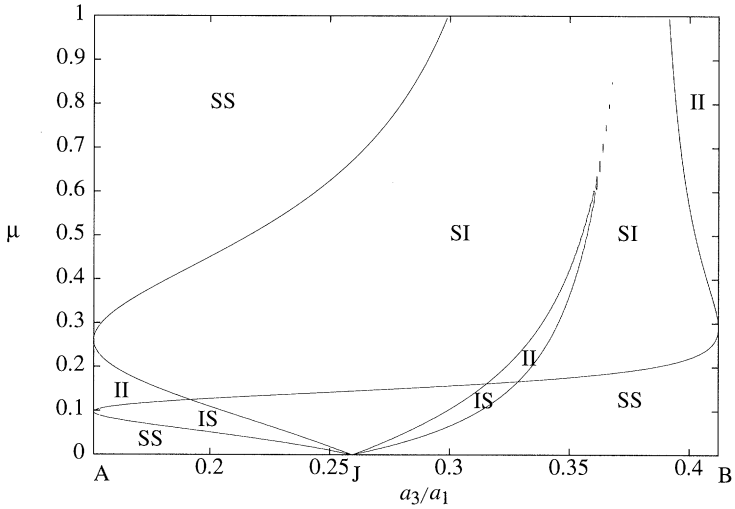

Figure 3. (*a*) The interval of wavevector orientations corresponding to instability for each permissible value of a_3/a_1, for $a_2/a_1 = 0.7$, from the least value $A = 0.2517$ where $x = 1$ to the greatest $B = 0.8143$, where $x = -1$. $J = 0.4781$ is the location of the Jacobi ellipsoid. The double letters identify regions in this diagram where the configurations are stable or unstable, the first of each double letter referring to the direct configuration, the second to the adjoint. For example, a region designated SI is a region of stability for the direct configurations but instability for the adjoint. Figure 3*b* shows the same for the value $a_2/a_1 = 0.3$, for which the corresponding values are $A = 0.1515$, $B = 0.4121$ and $J = 0.2594$. The irregularly dashed line in the lower left reflects a secondary instability tongue too narrow to be resolved (cf. figure 2).

grangian displacement $\boldsymbol{\xi}$ because its vanishing does not imply that $\boldsymbol{\xi}$ vanishes. This is because there exist particle-relabelling perturbations, insignificant physically, for which $\boldsymbol{\xi} \neq \mathbf{0}$ but for which the Eulerian perturbation $\boldsymbol{u}$ of the fluid velocity vanishes identically. This functional therefore measures precisely the contribution to the Lagrangian displacement that is physically significant. One can show that the mixed

(*a*)

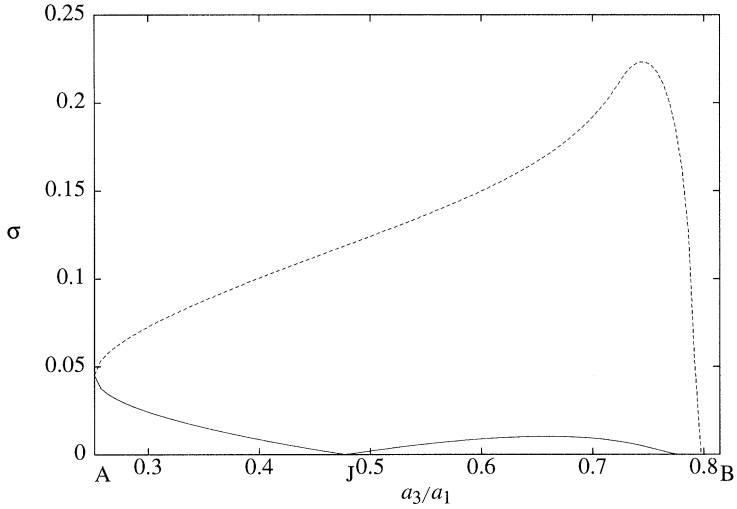

(*b*)

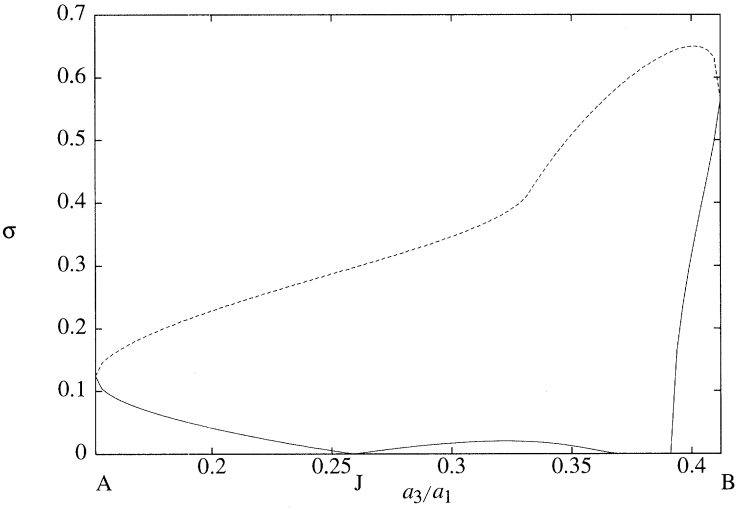

Figure 4. (*a*) The growth rate σ (maximized with respect to μ) for each permissible value of a_3/a_1 for $a_2/a_1 = 0.7$. The full line represents the values for the direct configurations, the dashed for the adjoint. Figure 4*b* shows the same for the value $a_2/a_1 = 0.3$.

Eulerian/Lagrangian representation of the perturbation equations may be viewed as fundamental by deriving a differential equation for $\xi_n|_{\partial D}$ as a function of time, from which it can be seen that the pair $(\boldsymbol{u}(\boldsymbol{x},t), \xi_n(\boldsymbol{x},t)|_{\partial D})$ are uniquely determined from their initial data. For this formulation $E^{1/2}$ becomes a genuine norm which was denoted in § 4 above by $\|(\boldsymbol{u},p)\|$. If E remains below some specified bound for sufficiently small initial data, we infer that the Eulerian velocity perturbation and the distortion of the free surface remain small, and therefore that the unperturbed configuration is stable (to the class of perturbations considered). Otherwise we infer instability.

We need an estimate for E when the evolution of $\boldsymbol{\xi}$ is governed by the *inhomoge-*

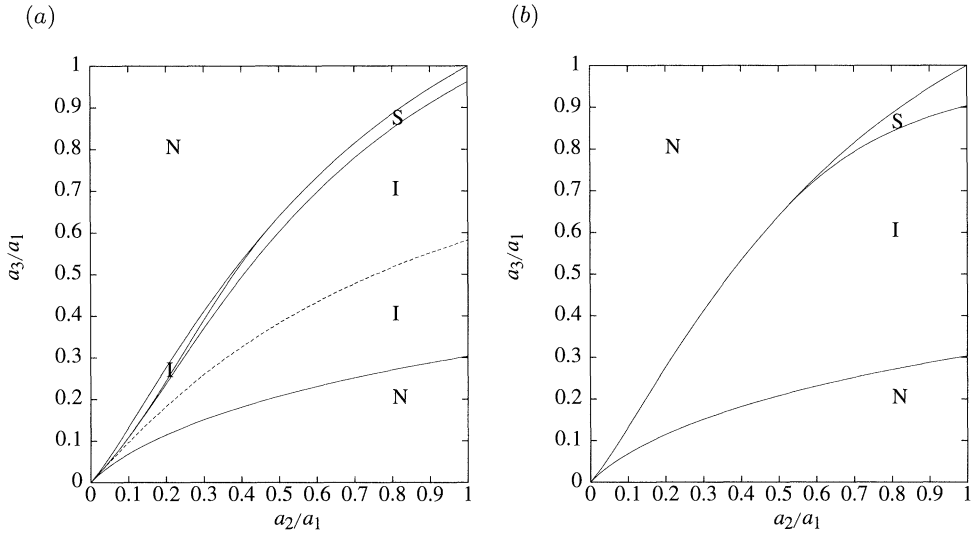

Figure 5. (*a*) Regions of stability (S) and instability (I) to short-wavelength perturbations for the direct configurations, in the $(a_2/a_1, a_3/a_1)$ plane. The thin stability band includes the upper bounding curve ($x = -1$) for $0.5 \leqslant a_2/a_1 \leqslant 1$ but separates from it for smaller values of a_2/a_1. Figure 5*b* shows the same for the adjoint configurations, for which the stability band exists only on the interval $0.5 \leqslant a_2/a_1 \leqslant 1$.

neous linearized equations

$$\frac{D\boldsymbol{u}}{Dt} + L\boldsymbol{u} + 2\Omega\boldsymbol{u} + \nabla p + \nabla\psi = \boldsymbol{F}, \tag{6.2}$$

$$\nabla \cdot \boldsymbol{u} = G. \tag{6.3}$$

When the Eulerian perturbations $\boldsymbol{u}$ and p represent the error terms in the geometrical-optics ansatz, the inhomogeneous terms $\boldsymbol{F}$ and G are given by equations (4.6) and (4.9). We seek the estimate in the form

$$\frac{\mathrm{d}E}{\mathrm{d}t} \leqslant CE + K \tag{6.4}$$

for some (sufficiently large) positive functions $C(t)$ and $K(t)$. This allows rapidly (e.g. exponentially) increasing E but is sufficient to validate the short-wavelength instability provided only that C and K can be chosen independent of the wavelength parameter ϵ. We use the symbol C to denote a positive number depending only on the unperturbed configuration and domain (and hence constant in our present application), the symbol K to denote a positive number having a time-dependence determined not only by that of the unperturbed configuration but also by that of the leading-order approximation $\boldsymbol{b}$.

We have introduced complex values for the dependent variables $\boldsymbol{u}$, p, etc., so each dependent variable is split into real and imaginary parts. For example,

$$\boldsymbol{u} = \boldsymbol{u}_{\mathrm{real}} + \mathrm{i}\boldsymbol{u}_{\mathrm{imag}}.$$

Since $|\boldsymbol{u}|^2 = |\boldsymbol{u}_{\mathrm{real}}|^2 + |\boldsymbol{u}_{\mathrm{imag}}|^2$ and $|\xi_n|^2 = |\xi_{n\mathrm{real}}|^2 + |\xi_{n\mathrm{imag}}|^2$, we find $E = E_{\mathrm{real}} + E_{\mathrm{imag}}$, where

$$E_{\mathrm{real}}(\boldsymbol{\xi}) = \frac{1}{2}\int_{D_t} |\boldsymbol{u}_{\mathrm{real}}(\boldsymbol{x}, t)|^2 \,\mathrm{d}\boldsymbol{x} + \frac{1}{2}\int_{\partial D_t} |\nabla P||\xi_{n\mathrm{real}}|^2 \,\mathrm{d}\sigma,$$

with a similar expression for E_{imag}. Suppose we can show that

$$\frac{\mathrm{d}E_{\text{real}}}{\mathrm{d}t} \leqslant CE_{\text{real}} + K \quad \text{and} \quad \frac{\mathrm{d}E_{\text{imag}}}{\mathrm{d}t} \leqslant CE_{\text{imag}} + K.$$

Then the sum E satisfies the same inequality with K replaced by $2K$, proving the estimate. Since the operators on the left-hand sides of equations (6.2) and (6.3) are real, splitting the right-hand sides into real and imaginary parts gives two sets of equations exactly like equations (6.2) and (6.3), but for the real and imaginary parts separately. We seek to verify inequality (6.4) for E_{real} and for E_{imag} separately. For this we may proceed under the assumption that all dependent variables are real. We now proceed to do so, dropping the subscripts 'real' and 'imag' (with one exception: it is less awkward to obtain the estimate (B 8) below for real and imaginary parts simultaneously).

Recalling that the outward normal to the surface ∂D_t is in the direction of $-\nabla P$, we see that the surface term in equation (6.1) may be rewritten. We have

$$\frac{\mathrm{d}E}{\mathrm{d}t} = \frac{\mathrm{d}}{\mathrm{d}t}\frac{1}{2}\int_{D_t} |\boldsymbol{u}(\boldsymbol{x},t)|^2\,\mathrm{d}\boldsymbol{x} - \frac{\mathrm{d}}{\mathrm{d}t}\frac{1}{2}\int_{\partial D_t} (\boldsymbol{\xi}\cdot\nabla P)\boldsymbol{\xi}\cdot\mathrm{d}\boldsymbol{\sigma}.$$

The time derivatives above may be taken inside the integrals with the aid of equations (A 1) and (A 3) in Appendix A. Applying these equations above gives

$$\frac{\mathrm{d}E}{\mathrm{d}t} = \int_{D_t} \boldsymbol{u}\cdot\frac{D\boldsymbol{u}}{Dt}\,\mathrm{d}x + \frac{1}{2}\int_{D_t} |\boldsymbol{u}(\boldsymbol{x},t)|^2\nabla\cdot\boldsymbol{V}\,\mathrm{d}x - \int_{\partial D_t} (\nabla P\cdot\boldsymbol{\xi})\boldsymbol{u}\cdot\,\mathrm{d}\boldsymbol{\sigma}$$
$$-\frac{1}{2}\int_{\partial D_t}\left\{(\boldsymbol{\xi}\cdot\nabla P)\nabla\cdot\boldsymbol{V} + \boldsymbol{\xi}\cdot\nabla\left(\frac{DP}{Dt}\right)\right\}\boldsymbol{\xi}\cdot\mathrm{d}\boldsymbol{\sigma}.$$

Replacing the term $D\boldsymbol{u}/Dt$ by its expression from equation (6.2), we find in place of the preceding equation

$$\frac{\mathrm{d}E}{\mathrm{d}t} = \int_{D_t} \boldsymbol{u}\cdot(-L\boldsymbol{u} - 2\boldsymbol{\omega}\times\boldsymbol{u} - \nabla p - \nabla\psi + \boldsymbol{F})\,\mathrm{d}\boldsymbol{x} + \frac{1}{2}\int_{D_t}(\nabla\cdot\boldsymbol{V})|\boldsymbol{u}|^2\,\mathrm{d}\boldsymbol{x}$$
$$+\int_{\partial D_t}|\nabla P|\xi_n u_n\,\mathrm{d}\sigma - \frac{1}{2}\int_{\partial D_t}\left((\boldsymbol{\xi}\cdot\nabla P)\nabla\cdot\boldsymbol{V} + \left(\boldsymbol{\xi}\cdot\nabla\frac{DP}{Dt}\right)\right)\boldsymbol{\xi}\cdot\,\mathrm{d}\boldsymbol{\sigma}.$$

The integral involving ∇p can be reduced with the aid of equations (2.9) and (6.3) as follows:

$$-\int_{D_t}(\boldsymbol{u}\cdot\nabla p)\,\mathrm{d}\boldsymbol{x} = \int_{D_t} pG\,\mathrm{d}\boldsymbol{x} - \int_{\partial D_t}|\nabla P|\xi_n u_n\,\mathrm{d}\sigma.$$

The expression for $\mathrm{d}E/\mathrm{d}t$ can be further reduced with the aid of the preceding expression and the observation that $\nabla(DP/Dt) = \phi\boldsymbol{n}$ where $\phi = \pm|\nabla(DP/Dt)|$. This is so because DP/Dt vanishes on ∂D_t. We now find

$$\frac{\mathrm{d}E}{\mathrm{d}t} = \int_{D_t}(\boldsymbol{u}\cdot(-L\boldsymbol{u} - 2\boldsymbol{\omega}\times\boldsymbol{u} + \boldsymbol{F}) + \tfrac{1}{2}(\nabla\cdot\boldsymbol{V})|\boldsymbol{u}|^2)\,\mathrm{d}\boldsymbol{x}$$
$$+\frac{1}{2}\int_{\partial D_t}(\phi - |\nabla P|\nabla\cdot\boldsymbol{V})\xi_n{}^2\,\mathrm{d}\sigma - \int_{D_t}(\boldsymbol{u}\cdot\nabla\psi - pG)\,\mathrm{d}\boldsymbol{x}.$$

We assume that the velocity field $\boldsymbol{V}$ and its first partial derivatives are bounded in the closure of the domain D_t. The function $\boldsymbol{F}$ is known from the explicit calculations of § 5 to be localized, bounded spatially and to have a time dependence like that

of the leading-order approximation $\boldsymbol{b}$. The inequality $2|\boldsymbol{u}\cdot\boldsymbol{F}| \leqslant |\boldsymbol{u}|^2 + |\boldsymbol{F}|^2$ may be applied to the term involving this function. This implies that the first integral on the right in the equation above is bounded above by a positive number times the integral of $|\boldsymbol{u}|^2 + |\boldsymbol{F}|^2$. We further assume that $|\nabla P|$ is bounded away from zero on the boundary ∂D_t and that $\phi = \pm|\nabla(DP/Dt)|$ is bounded there. Then the second integral on the right is bounded by a positive number times the integral over ∂D_t of $|\nabla P|{\xi_n}^2$. This implies that

$$\frac{\mathrm{d}E}{\mathrm{d}t} \leqslant C_0 E + K_0 - \int_{D_t} \boldsymbol{u}\cdot\nabla\psi\,\mathrm{d}\boldsymbol{x} + \int_{D_t} pG\,\mathrm{d}\boldsymbol{x}, \tag{6.5}$$

where C_0 depends only on the unperturbed configuration (and is time-dependent if D_t is); K_0 has a time-dependence inherited from $\boldsymbol{F}$. The assumptions used above are easily verified for the Riemann ellipsoids.

Estimates for the integrals on the right-hand side of (6.5) are provided by classical potential theory. These estimates are easiest to state if we introduce the notations

$$||f||_D = \left(\int_D |f|^2\,\mathrm{d}\boldsymbol{x}\right)^{1/2}, \tag{6.6}$$

$$||f||_{\partial D} = \left(\int_{\partial D} |f|^2\,\mathrm{d}\sigma\right)^{1/2}, \tag{6.7}$$

where the single vertical bars sign can mean either the absolute value of a scalar or the norm of a three-component vector. The estimates in question are inequalities (B 1) and (B 2), derived in Appendix B. Since we are assuming that $c^{-1} < |\nabla P|_{\partial D} < c$ for some positive constant c, we can rewrite these estimates as follows

$$||\nabla\psi||_D \leqslant CE, \tag{6.8}$$

and

$${||p||_D}^2 \leqslant C'E + K'. \tag{6.9}$$

Applying them now in inequality (6.5) we can obtain the estimate (6.4). Consider the second term on the right-hand side of (6.5). With the aid of the Cauchy–Schwartz inequality we find

$$\left|\int_D \boldsymbol{u}\cdot\nabla\psi\,\mathrm{d}\boldsymbol{x}\right| \leqslant ||\boldsymbol{u}||_D||\nabla\psi||_D \leqslant C||\boldsymbol{u}||_D||\xi_n||_{\partial D} \leqslant C_1 E,$$

where we have observed that each of the terms in the penultimate expression on the right is less than a constant times $E^{1/2}$. Similarly, recalling that the function G is bounded spatially for each fixed t, we obtain

$$\left|\int_D pG\,\mathrm{d}\boldsymbol{x}\right| \leqslant \frac{1}{2}\int_D (|p|^2 + |G|^2)\,\mathrm{d}\boldsymbol{x} \leqslant C''E + K''.$$

This now gives (6.4).

7. Discussion

The analysis of the linear stability of the S-type Riemann ellipsoids has been extended to include disturbances of arbitrarily short wavelength. This can be viewed as supplementing the normal-mode analyses of these configurations. An apparent

PHILOSOPHICAL TRANSACTIONS OF THE ROYAL SOCIETY A MATHEMATICAL, PHYSICAL & ENGINEERING SCIENCES

technical difference in the analyses is that perturbations of the free surface, and therefore of the gravitational potential, play no role in our analysis, while they play an important role in the normal-mode analysis (Chandrasekhar 1969). We have not, however, ignored these perturbations, but rather have set them equal to zero initially, and verified that their subsequent role is insignificant. We believe (but have not explicitly verified) that allowing for them initially would create contributions of order ϵ^2 in the linearized stability equations, and would therefore play no role in the stabilty analysis. In words, the perturbation of the gravitational potential is negligible for perturbations of short wavelength. The normal-mode analyses of these configurations are surprisingly incomplete, being largely restricted to surface harmonics of order three (and, in isolated cases, of order four). We anticipate that when the parameter space of the Riemann ellipsoids is explored for normal modes of higher wavelength, the effects of the self-gravitational perturbation will become increasingly less.

The present analysis shows that very little of the parameter space represents stable configurations; if stability analyses at longer wavelengths are carried out, one may find that even less of the parameter space remains stable. The circumstance that most of the S-type Riemann ellipsoids are unstable to disturbances of short wavelength raises a number of physical questions.

Among near-axisymmetric configurations, only those that are not too distorted from the spherical are stable to perturbations of short wavelength. Evolutionary scenarios for stars and planets typically involve quasistatic phases of slow evolution. If a fluid mass evolves slowly through a family of S-type ellipsoids and encounters the parameter domain of unstable configurations, the velocity field can no longer remain that of elliptical streamlines normally associated with these configurations, but must become complicated. The result will be a kind of turbulence drawing its energy, not from thermal sources, but from the shear. This mechanism for producing turbulence is one of the motivations for the study of three-dimensional disturbances of two-dimensional flows (cf. Bayly *et al.* 1988). It is not clear whether it can be an effective transport mechanism in stellar or planetary interiors: the basis for our linear analysis is that, in leading order, the disturbance can be localized near a given set of streamlines, so there is no transport in this limit. Whether this localization would persist in a nonlinear treatment is not known. This is a question of considerable importance in the theory of stellar evolution, where it is normally assumed that very little mixing of material takes place in thermally stable stellar interiors. The idea that this mechanism may be at work in tidally distorted planets and stars is a very natural one (Malkus 1993) in view of the tidal distortion of streamlines.

Since the emphasis in this paper has been on small wavelengths, the effect of viscosity can be important. It has been considered in the setting of an unbounded flow by Craik & Criminale (1986), Landman & Saffman (1987) and others (see Greenspan 1990). They find a damping effect essentially proportional to $\exp(-\nu \int k^2 \, \mathrm{d}t)$, where ν is the coefficient of kinematic viscosity, as one would expect. This simply multiplies the solution obtained from the inviscid analysis. The result is that when the latter analysis predicts instability, the instability will be damped out if its growth rate is less than νk^2, but will persist otherwise. For the stellar case, where extremely small kinematic viscosities are expected, there may well be instabilities in wavelength regimes that survive the effect of viscosity. Furthermore, the only stable parameter domain is that provided by the rotational stabilization of flows that would otherwise be unstable. Gyroscopic stablization is known in other cases to be destroyed by dissipation. Viscosity may therefore in fact play a *destabilizing* role.

PHILOSOPHICAL TRANSACTIONS OF THE ROYAL SOCIETY A MATHEMATICAL, PHYSICAL & ENGINEERING SCIENCES

We thank Peter Constantin, David Levermore and Carlos Kenig for their advice and help. This work was supported by the National Science Foundation through grants number DMS92078080 with the University of Chicago (N.R.L.) and IRI9924605 with the University of Illinois at Chicago (A.L.).

Appendix A. Differentiation of integrals

We have encountered in the text of this article integrals extended over time-dependent spatial domains. Such integrals are common in continuum mechanics, and there are formulas for their derivatives when the dependence of the domain on t arises as follows. Let $\boldsymbol{x} = \boldsymbol{X}(\boldsymbol{x}_0, t)$ be the solution of the initial-value problem

$$\frac{\mathrm{d}\boldsymbol{x}}{\mathrm{d}t} = \boldsymbol{V}(\boldsymbol{x}, t), \quad \boldsymbol{x}|_{t=0} = \boldsymbol{x}_0.$$

Denote by D_t the image of an initial, three-dimensional domain D_0 under the mapping $\boldsymbol{X}$: $D_t = \boldsymbol{X}(D_0, t)$. Likewise, given an initial two-dimensional surface S_0 in three-dimensional space, denote by S_t its image under $\boldsymbol{X}$. In the applications above $S_t = \partial D_t$, but this plays no role in the following two formulas. Let f and $\boldsymbol{A}$ be arbitrary, smooth scalar and vector (respectively) functions of position and time. Then (see Truesdell 1954)

$$\frac{\mathrm{d}}{\mathrm{d}t}\int_{D_t} f\,\mathrm{d}\boldsymbol{x} = \int_{D_t}\left(\frac{Df}{Dt} + f\nabla\cdot\boldsymbol{V}\right)\mathrm{d}\boldsymbol{x} \tag{A 1}$$

and

$$\frac{\mathrm{d}}{\mathrm{d}t}\int_{S_t}\boldsymbol{A}\cdot\mathrm{d}\boldsymbol{\sigma} = \int_{S_t}\left(\frac{D\boldsymbol{A}}{Dt} - (\boldsymbol{A}\cdot\nabla)\boldsymbol{V} + \boldsymbol{A}\nabla\cdot\boldsymbol{V}\right)\cdot\mathrm{d}\boldsymbol{\sigma}. \tag{A 2}$$

In the text we use equation (A 1) and the following consequence of equation (A 2):

Lemma A.1. *Let $P(\boldsymbol{x}, t)$ be constant on S_t. Define*

$$\boldsymbol{u} = \frac{D\boldsymbol{\xi}}{Dt} - (\boldsymbol{\xi}\cdot\nabla)\boldsymbol{V}.$$

Then

$$\frac{\mathrm{d}}{\mathrm{d}t}\int_{S_t}(\boldsymbol{\xi}\cdot\nabla P)\boldsymbol{\xi}\cdot\mathrm{d}\boldsymbol{\sigma} = 2\int_{S_t}(\boldsymbol{\xi}\cdot\nabla P)\,\boldsymbol{u}\cdot\mathrm{d}\boldsymbol{\sigma} + \int_{S_t}\left((\boldsymbol{\xi}\cdot\nabla P)\nabla\cdot\boldsymbol{V} + \boldsymbol{\xi}\cdot\nabla\left(\frac{DP}{Dt}\right)\right)\boldsymbol{\xi}\cdot\mathrm{d}\boldsymbol{\sigma}. \tag{A 3}$$

To prove this, put $\boldsymbol{A} = (\boldsymbol{\xi}\cdot\nabla P)\boldsymbol{\xi}$ in equation (A 2) above. The integrand of the right-hand side of that formula becomes

$$(\boldsymbol{\xi}\cdot\nabla P)\left(\frac{D\boldsymbol{\xi}}{Dt} - (\boldsymbol{\xi}\cdot\nabla)\,\boldsymbol{V} + \boldsymbol{\xi}\nabla\cdot\boldsymbol{V}\right) + \left(\frac{D\boldsymbol{\xi}}{Dt}\cdot\nabla P + \boldsymbol{\xi}\cdot\left(\frac{D}{Dt}\nabla P\right)\right)\boldsymbol{\xi}.$$

Using the definition of $\boldsymbol{u}$ and rearranging, we find

$$(\boldsymbol{\xi}\cdot\nabla P)\,\boldsymbol{u} + (\boldsymbol{u}\cdot\nabla P)\,\boldsymbol{\xi} + \left((\boldsymbol{\xi}\cdot\nabla P)\,\nabla\cdot\boldsymbol{V} + \boldsymbol{\xi}\cdot\nabla\left(\frac{DP}{Dt}\right)\right)\boldsymbol{\xi},$$

PHILOSOPHICAL TRANSACTIONS OF THE ROYAL SOCIETY A MATHEMATICAL, PHYSICAL & ENGINEERING SCIENCES

where we have further observed the identity

$$\boldsymbol{\xi}\cdot\frac{D}{Dt}\nabla P+\nabla P\cdot((\boldsymbol{\xi}\cdot\nabla)\,\boldsymbol{V})=\boldsymbol{\xi}\cdot\nabla\left(\frac{DP}{Dt}\right). \tag{A 4}$$

We now have the formula

$$\frac{\mathrm{d}}{\mathrm{d}t}\int_{S_t}(\boldsymbol{\xi}\cdot\nabla P)\,\boldsymbol{\xi}\cdot\mathrm{d}\boldsymbol{\sigma}=\int_{S_t}((\nabla P\cdot\boldsymbol{\xi})\,\boldsymbol{u}+(\nabla P\cdot\boldsymbol{u})\,\boldsymbol{\xi})\cdot\mathrm{d}\boldsymbol{\sigma}$$
$$+\int_{S_t}\left((\boldsymbol{\xi}\cdot\nabla P)\,\nabla\cdot\boldsymbol{V}+\boldsymbol{\xi}\cdot\nabla\left(\frac{DP}{Dt}\right)\right)\boldsymbol{\xi}\cdot\mathrm{d}\boldsymbol{\sigma}.$$

Since $\nabla P=\pm|\nabla P|\boldsymbol{n}$ where $\boldsymbol{n}$ is normal to S_t, each of the first two integrands on the right is equal to $\pm\xi_n u_n|\nabla P|$. This gives equation (A 3) of the Lemma.

Appendix B. Estimates from potential theory

The following estimates

$$||\nabla\psi||_D\leqslant C||\xi_n||_{\partial D}, \tag{B 1}$$

and

$$||p||_D{}^2\leqslant C'(||\boldsymbol{u}||_D{}^2+||\xi_n||_{\partial D}{}^2)+K' \tag{B 2}$$

needed in § 6 are proved in this appendix.

Consider first the estimate (B 1), with f in place of ξ_n for brevity:

$$\psi(\boldsymbol{x})=\frac{1}{\pi}\int_{\partial D}\frac{f(\boldsymbol{y})}{|\boldsymbol{x}-\boldsymbol{y}|}\,\mathrm{d}\sigma_y.$$

We have, for $\boldsymbol{x}\in D$ and $0<\epsilon<1/2$,

$$|\nabla\psi(\boldsymbol{x})|\leqslant\frac{1}{\pi}\int_{\partial D}\frac{|f(\boldsymbol{y})|}{|\boldsymbol{x}-\boldsymbol{y}|^2}\,\mathrm{d}\sigma_y=\frac{1}{\pi}\int_{\partial D}\frac{1}{|\boldsymbol{x}-\boldsymbol{y}|^{1-\epsilon}}\frac{|f(\boldsymbol{y})|}{|\boldsymbol{x}-\boldsymbol{y}|^{1+\epsilon}}\,\mathrm{d}\sigma_y.$$

Therefore, by the Schwarz inequality,

$$|\nabla\psi(\boldsymbol{x})|^2\leqslant\frac{1}{\pi^2}\int_{\partial D}\frac{\mathrm{d}\sigma_y}{|\boldsymbol{x}-\boldsymbol{y}|^{2-2\epsilon}}\int_{\partial D}\frac{|f(\boldsymbol{y})|^2}{|\boldsymbol{x}-\boldsymbol{y}|^{2+2\epsilon}}\,\mathrm{d}\sigma_y\leqslant C_0\int_{\partial D}\frac{|f(\boldsymbol{y})|^2}{|\boldsymbol{x}-\boldsymbol{y}|^{2+2\epsilon}}\,\mathrm{d}\sigma_y,$$

since the first integral in the middle term is bounded in D for $\epsilon>0$. Integrating either side over D, we obtain

$$||\nabla\psi||_D{}^2=\int_D|\nabla\psi\,(\boldsymbol{x})|^2\,d\boldsymbol{x}\leqslant C_0\int_D\int_{\partial D}\frac{f(\boldsymbol{y})^2}{|\boldsymbol{x}-\boldsymbol{y}|^{2+2\epsilon}}\,\mathrm{d}\sigma_y\,\mathrm{d}\boldsymbol{x}$$
$$=C_0\int_{\partial D}f(\boldsymbol{y})^2\left(\int_D\frac{\mathrm{d}\boldsymbol{x}}{|\boldsymbol{x}-\boldsymbol{y}|^{2+2\epsilon}}\right)\mathrm{d}\sigma_y\leqslant C_2||f||_{\partial D}{}^2,$$

since the inner integral in the last expression is bounded for $\boldsymbol{y}\in D$ as long as $\epsilon<1/2$. This proves the estimate in question.

Turning now to the estimate (B 2), we first obtain a Poisson equation for the Eulerian pressure-perturbation p by taking the divergence of each side of equation (6.2). The boundary condition is given by equation (2.9). Next we split p into the sum p_1+p_2 where p_1 and p_2 satisfy the potential problems

$$\Delta p_1=0,\qquad p_1|_{\partial D}=|\nabla P|\,f|_{\partial D}, \tag{B 3}$$

and

$$\Delta p_2 = g(\boldsymbol{x}, t), \quad p_2|_{\partial D} = 0, \tag{B 4}$$

where

$$g = \nabla \cdot \left(\boldsymbol{F} - \frac{D\boldsymbol{u}}{Dt} - L\boldsymbol{u} - 2\boldsymbol{\omega} \times \boldsymbol{u} \right), \tag{B 5}$$

and we continue to write f in place of ξ_n.

Consider first equation (B 3). Let Γ be the Green's function for the solution to this problem:

$$\begin{aligned} |p_1(\boldsymbol{x})| &= \left| \int_{\partial D} \Gamma(\boldsymbol{x}, \boldsymbol{y}) \, |\nabla P(\boldsymbol{y})| \, f(\boldsymbol{y}) \, \mathrm{d}\sigma_y \right| \\ &\leqslant \int_{\partial D} \Gamma(\boldsymbol{x}, \boldsymbol{y})^{1/2} \Gamma(\boldsymbol{x}, \boldsymbol{y})^{1/2} \, |\nabla P(\boldsymbol{y})| \, |f(\boldsymbol{y})| \, \mathrm{d}\sigma_y, \end{aligned}$$

where we have used the fact that Γ is positive on D. By the Schwarz inequality,

$$|p_1(\boldsymbol{x})|^2 \leqslant \int_{\partial D} \Gamma(\boldsymbol{x}, \boldsymbol{y}) \, \mathrm{d}\sigma_y \int_{\partial D} \Gamma(\boldsymbol{x}, \boldsymbol{y}) \, |\nabla P(\boldsymbol{y})|^2 \, |f(\boldsymbol{y})|^2 \, \mathrm{d}\sigma_y.$$

The first factor is the function harmonic in D and taking the value unity on the boundary, hence is unity throughout. Now integrating each side over D, we obtain

$$||p_1||_D{}^2 \leqslant \int_{\partial D} \left(\int_D \Gamma(\boldsymbol{x}, \boldsymbol{y}) \, \mathrm{d}\boldsymbol{x} \right) |\nabla P(\boldsymbol{y})|^2 \, |f(\boldsymbol{y})|^2 d\sigma_y \leqslant C_3 ||f||_{\partial D}{}^2, \tag{B 6}$$

for some constant C_3. Here we have used the fact that the inner integral is bounded on D (it is continuous on the closure of D), and that $|\nabla P|$ is bounded on ∂D.

Next consider equation (B 4). We note from equation (B 5) that the function g includes a term involving a time-derivative of $\boldsymbol{u}$. We use the identity, valid if $\nabla \cdot \boldsymbol{V} = 0$ (cf. equation (A 4) above from which it follows),

$$\nabla \cdot \frac{D\boldsymbol{u}}{Dt} - \frac{D}{Dt} \nabla \cdot \boldsymbol{u} = \nabla \cdot (L\boldsymbol{u}).$$

Note that the function G of equation (6.3) above has the structure $G = G_1 \mathrm{e}^{\mathrm{i}\Phi/\epsilon}$ where G_1 is spatially localized and bounded, and has the same time-dependence as $\boldsymbol{u}^{(0)}$. Referring to equation (4.11), we now find for equation (B 5)

$$g = \mathrm{e}^{\mathrm{i}\Phi/\epsilon} G_2 + \nabla \cdot (\boldsymbol{F} - 2L\boldsymbol{u} - 2\boldsymbol{\omega} \times \boldsymbol{u}), \tag{B 7}$$

where $G_2 = DG_1/Dt$, hence is also bounded and localized.

Since p_2 vanishes on ∂D, we find (retaining the complex form, which is less awkward in this case)

$$\begin{aligned} ||\nabla p_2||_D{}^2 &= \int_D \nabla p_2^* \cdot \nabla p_2 \, \mathrm{d}\boldsymbol{x} = -\int_D p_2^* \Delta p_2 \, \mathrm{d}\boldsymbol{x} \\ &= -\int_D p_2^* \mathrm{e}^{\mathrm{i}\Phi/\epsilon} \, G_2 \, \mathrm{d}\boldsymbol{x} - \int_D p_2^* \nabla \cdot (F - 2L\boldsymbol{u} - 2\boldsymbol{\omega} \times \boldsymbol{u}) \, \mathrm{d}\boldsymbol{x} \\ &= -\int_D p_2^* \mathrm{e}^{\mathrm{i}\Phi/\epsilon} \, G_2 \, \mathrm{d}\boldsymbol{x} + \int_D (\nabla p_2^*) \cdot (F - 2L\boldsymbol{u} - 2\boldsymbol{\omega} \times \boldsymbol{u}) \, \mathrm{d}\boldsymbol{x}, \end{aligned}$$

or

$$||\nabla p_2||_D{}^2 \leqslant \int_D |p_2||G_2| \, d\boldsymbol{x} + \int_D |\nabla p_2||F| \, \mathrm{d}\boldsymbol{x} + C \int_D |\nabla p_2||\boldsymbol{u}| \, \mathrm{d}\boldsymbol{x}. \tag{B 8}$$

We now make repeated use of the inequality

$$2ab \leqslant \frac{1}{\mu}a^2 + \mu b^2$$

valid for arbitrary positive numbers a, b, μ. Inequality (B 8) becomes

$$||\nabla p_2||_D{}^2 \leqslant \tfrac{1}{2}\mu||p_2||_D{}^2 + \tfrac{1}{2}(\mu^{-1}||G_2||_D{}^2 + \mu||\nabla p_2||_D{}^2 + \mu^{-1}||F||_D{}^2)$$
$$+\tfrac{1}{2}(\mu C||\nabla p_2||_D{}^2 + C\mu^{-1}||\boldsymbol{u}||_D{}^2).$$

For small enough μ this implies that

$$||\nabla p_2||_D{}^2 \leqslant \tfrac{1}{2}\mu C_4||p_2||_D{}^2 + C_5||\boldsymbol{u}||_D^2 + K_1,$$

where K_1 is proportional to

$$\int_D (|G_2|^2 + |F|^2)\,\mathrm{d}\boldsymbol{x}$$

and therefore grows in time like $|\boldsymbol{a}|^2$.

Now Poincaré's inequality

$$||p_2||_D{}^2 \leqslant C_6||\nabla p_2||_D{}^2$$

implies (after again exploiting the arbitrariness of μ)

$$||p_2||_D{}^2 \leqslant C_7||\boldsymbol{u}||_D{}^2 + K_2.$$

Combining this with inequality (B 1) above now gives

$$||p||_D{}^2 = ||p_1 + p_2||_D{}^2 \leqslant 2(||p_1||_D{}^2 + ||p_2||_D{}^2) \leqslant 2C_7||\boldsymbol{u}||_D{}^2 + 2K_2 + 2C_3||f||_{\partial D}{}^2,$$

which is equivalent to inequality (B 2).

References

Bayly, B. J. 1986 Three-dimensional instability of elliptical flow. *Phys. Rev. Lett.* **57**, 2160–2163.

Bayly, B. B., Orszag, S. A. & Herbert, T. 1988 Instability mechanisms in shear-flow transition *A. Rev. Fluid Mech.* **20**, 359–391.

Bayly, B. B., Holm, D. D. & Lifschitz, A. 1996 Three-dimensional stability of elliptical vortex columns in external strain flows. *Phil. Trans. R. Soc. Lond* A **354**, 895–926. (Preceding paper.)

Chandrasekhar, S. 1969 *Ellipsoidal figures of equilibrium.* New Haven, CT: Yale University Press.

Craik, A. D. D. 1989 The stability of unbounded two- and three-dimensional flows subject to body forces: some exact solutions. *J. Fluid Mech.* **198**, 275–292.

Craik, A. D. D. & Criminale, W. O. 1986 Evolution of wavelike disturbances in shear flows: a class of exact solutions of the Navier–Stokes equations. *Proc. R. Soc. Lond.* A **406**, 13–26.

Eckhoff, K. S. 1981 On the stability for symmetric hyperbolic systems. I. *J. diffl Equats* **40**, 94–115.

Gledzer, E. B. & Ponomarev, V. M. 1992 Instability of bounded flows with elliptical streamlines. *J. Fluid Mech.* **240**, 1–30.

Greenspan, H. 1990 *Theory of rotating fluids.* Brookline, MA: Breukelen.

Landman, M. J. & Saffman, P. G. 1987 The three-dimensional instability of strained vortices in a viscous fluid. *Phys. Fluids* **30**, 2339–2342.

Lebovitz, N. R. 1979 Ellipsoidal potentials of polynomial distributions of matter. *Astrophys. J.* **234**, 619–627.

Lebovitz, N. R. 1989 Lagrangian perturbations of Riemann ellipsoids. *Astrophys. Geophys. Fluid Dyn.* **47**, 225–236.

Lifschitz, A. & Hameiri, E. 1991 Local stability conditions in fluid dynamics. *Phys. Fluids* A **3**, 2644–2651.

Magnus, W. & Winkler, S. 1979 *Hill's equation.* New York: Dover.

Malkus, W. 1993 *Theory of solar and planetary dynamos.* In *Proc. NATO Adv. Stud. Inst.*, ch. 5. Cambridge University Press.

Pierrehumbert, R. T. 1986 Universal short-wave instability of two-dimensional eddies in an inviscid fluid. *Phys. Rev. Lett.* **57**, 2157–2159.

Riemann, B. 1860 Ein Beitrag zu den Untersuchengen über die Bewegung eines flüssigen gleichartigen Ellipsoides. *Gött. Abh.* **IX**, 3–36.

Truesdell, C. 1954 *The kinematics of vorticity.* Bloomington: Indiana University.

Vladimirov, V. A. & Vostretsov, D. G. 1986 Instability of steady flows with constant vorticity in vessels of elliptic cross-section. *Prikl. Math. Mech. USSR* **50**, 279–285.

Waleffe, F. 1990 On the three-dimensional instability of strained vortices. *Phys. Fluids* A **2**, 76–80.

Received 4 January 1994; revised 6 September 1994; accepted 19 April 1995

PHILOSOPHICAL TRANSACTIONS OF THE ROYAL SOCIETY A MATHEMATICAL, PHYSICAL & ENGINEERING SCIENCES